JACS
JOURNAL OF THE AMERICAN CHEMICAL SOCIETY
Article
pubs.acs.org/JACS

Studies on a "Disappearing Polymorph": Thermal and Magnetic Characterization of α-*p*-$NCC_6F_4CNSSN^{\bullet}$

Yassine Beldjoudi,[†] Ana Arauzo,[‡] Fernando Palacio,*[,‡] Melanie Pilkington,[§] and Jeremy M. Rawson*[,†]

[†]Department of Chemistry & Biochemistry, University of Windsor, 401 Sunset Avenue, Windsor, OntarioN9B 3P4, Canada
[‡]Departamento de Física de la Materia Condensada, Facultad de Ciencias, and Instituto de Ciencia de Materiales de Aragon, CSIC-Universidad de Zaragoza, E-50009 Zaragoza, Spain
[§]Department of Chemistry, Brock University, 1812 Sir Isaac Brock Way, St. Catharines, Ontario L2S 3A1, Canada

Supporting Information

ABSTRACT: The α-and β-phases of the thiazyl radical *p*-$NCC_6F_4CNSSN^{\bullet}$ (**1**) can be selectively prepared by careful control of the sublimation conditions, with the α-phase crystallizing preferentially when the substrate temperature is maintained below −10 °C, whereas the β-phase is isolated when the substrate temperature is maintained at or above ambient temperature. Differential scanning calorimetry studies reveal that the α-phase converts to the β-phase upon warming over the range 111−117 °C (ΔH = +4 kJ·mol^{-1}) via a melt−recrystallization process, with the β-phase itself melting at 167−170 °C (ΔH_{fus} = 27 kJ·mol^{-1}). IR and Raman spectroscopy can be used to clearly discriminate between **1**$\boldsymbol{\alpha}$ and **1**$\boldsymbol{\beta}$. The α-phase shows a broad maximum in the magnetic susceptibility around 8 K that, coupled with a broad maximum in the heat capacity, is indicative of short-range order. Some field dependence of the susceptibility below 3 K is observed, but the lack of features in the ac susceptibility, *M* vs *H* plots, or heat capacity mitigates against long-range order in **1**$\boldsymbol{\alpha}$.

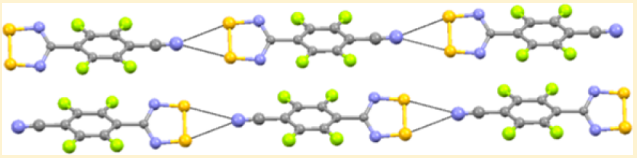

INTRODUCTION

The discovery of ferromagnetism at 0.65 K in the β-phase of *p*-nitrophenyl nitronylnitroxide (*p*-NPNN) in 1993 heralded a new era in magnetism.[1] The observation of a spontaneous magnetic moment in a system containing unpaired electrons in *p*-orbitals was in stark contrast to observations with other magnetic materials, in which the unpaired electrons were located in the *d*- or *f*-orbitals associated with transition metals, lanthanides and actinides. Since then, considerable efforts have been made to develop other "organic" magnets. Much of the original work focused on tuning the functionality of nitroxide and nitronylnitroxide radicals and led to a series of derivatives that typically exhibited long-range order below 4 K.[2] During that period, Wudl and co-workers reported that the fullerene charge-transfer salt C_{60}·TDAE (TDAE = tetrakis(dimethylamino)ethylene) ordered at 16 K, indicating that substantially higher magnetic ordering temperatures could be accessible for such light-atom systems.[3] Around that time, work in our laboratories focused on the development of thiazyl (S/N)-based radicals that we felt may offer some potential benefits in the field of organic molecular magnetism. Specifically, several families of sterically unencumbered thiazyl radicals were known, which offered the potential for dispersion-driven S···S or electrostatically favorable $S^{\delta+}\cdots N^{\delta-}$ close contacts between regions of spin density.[4] We believed that such close contacts coupled with the radially expanded orbitals of S should enhance magnetic exchange, favoring higher magnetic ordering temperatures. In addition, the incorporation of heavier *p*-block elements should give rise to larger spin−orbit coupling (dependent upon Z^4)[5] that, in turn, should lead to enhanced magnetic anisotropy and larger coercive fields.[6] The β-phase of the dithiadiazolyl radical *p*-$NCC_6F_4CNSSN^{\bullet}$ (**1**) was found to exhibit weak ferromagnetism (canted antiferromagnetism) at 36 K at ambient pressure,[7] increasing to 70 K under pressure.[8] More recent studies by Oakley on a series of resonance-stabilized bis(dithiazolyl) radicals have fully vindicated this approach with a series of reports on canted antiferromagnets and ferromagnets with ordering temperatures up to 35 K and coercive fields in excess of 1 T.[6a] In addition, Fujita and Awaga reported ferromagnetism in the radical cation salt [BBDTA]-[$GaCl_4$] at 6.7 K,[9] as well as antiferromagnetism in a paramagnetic phase of BDTA at 11 K.[10]

Initial studies on radical **1** revealed that it crystallized in the space group $P\bar{1}$, with molecules adopting a chain-like structure in the solid state, linked via structure-directing[11] $CN^{\delta-}\cdots S^{\delta+}$ interactions, with the presence of the crystallographic inversion center leading to antiparallel chain alignment.[12] Preliminary magnetic measurements revealed a broad maximum in χ around 8 K, consistent with short-range antiferromagnetic order, but subsequent studies revealed a broad maximum in χ around 60 K, with strongly field-dependent behavior below 36 K. This dichotomy was resolved with the discovery that **1** is polymorphic: phase **1**$\boldsymbol{\alpha}$ (triclinic, $P\bar{1}$) exhibited weak antiferromagnetic interactions, reflected in a broad maximum in χ around 8 K, whereas **1**$\boldsymbol{\beta}$ (orthorhombic, *Fdd*2)[6] exhibited stronger antiferromagnetic[13] interactions, reflected in a broad maximum in χ around 60 K and an ordered spin-canted

Received: October 17, 2016
Published: December 1, 2016

ACS Publications © 2016 American Chemical Society

DOI: 10.1021/jacs.6b10707
J. Am. Chem. Soc. 2016, 138, 16779−16786

antiferromagnetic structure below 36 K. The onset of long-range order in **1β** is accompanied by a small λ-type anomaly in the heat capacity in the vicinity of T_c, an out-of-phase component in the ac susceptibility, and enhancement of selected reflections in powder neutron diffraction experiments.[14] Measurement of the temperature dependence of the spontaneous magnetization (M_s (H = 0)), as well as electron paramagnetic resonance (EPR), spin relaxation (μ-SR), and resonant ultrasound spectroscopy (RUS), all reveal a classical saturation of the sublattice magnetization below 36 K.[15]

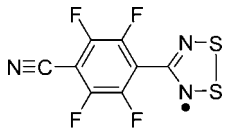

Compound 1

Polymorphism in molecular magnetic materials is not an uncommon phenomenon and has a marked effect on the solid-state magnetic properties.[16] While the magnetic behavior of **1β** in itself has proved exceptionally interesting, the apparent disappearance of the α-phase in our hands proved particularly exacerbating and has hampered a detailed study of its magnetic behavior. While the phenomenon of "disappearing polymorphs" is not without precedence,[17] occasional "guest appearances" by **1α**, usually in small quantities in the hands of less experienced students in our laboratories, has driven us to investigate the polymorphism in **1**. In this paper, we report an improved synthesis of **1**, identify the conditions necessary to selectively prepare both **1α** and **1β**, and examine the conversion of **1α** to **1β** through a combination of powder X-ray diffraction (PXRD), differential scanning calorimetry (DSC), and hot-stage microscopy measurements. We also examine the use of IR and Raman spectroscopies to distinguish **1α** from **1β** and undertake the first detailed magnetic characterization of **1α**.

EXPERIMENTAL SECTION

Solid-state Raman spectra were recorded on a Renishaw *inVia* Raman microscope using the excitation of the 785 nm laser lines, whereas IR spectra were recorded on a Bruker Alpha-P FT-IR instrument in the ATR geometry with a diamond ATR unit. Solution EPR spectra were recorded on a Bruker EMXplus EPR spectrometer at room temperature in dry CH_2Cl_2. DSC studies were performed on a Mettler Toledo DSC 822e instrument. Nitrogen was used to purge the system at a flow rate of 60 mL·min^{-1}. Samples were run in closed crucibles from −10 to 200 °C at a rate of 10 °C·min^{-1} on heating and a slower cooling rate of 5 °C·min^{-1} due to the formation of metastable glassy states, which appears common for many of these radicals.[18] Temperature ranges for melting or phase transitions are quoted as onset to peak maximum. Hot-stage optical microscopy experiments were performed on an Olympus BX51 microscope using an HCS402 Instec hot stage connected to a STC 200 temperature controller under an inert atmosphere. The micrographs of **1α** and **1β** were recorded at 10× magnification using a camera attached to the microscope. Powder X-ray diffraction (PXRD) patterns (30 min exposure) were collected using a Bruker D8 Discover diffractometer equipped with a Hi-Star area detector and GADDS software package using Cu Kα_1 radiation (40 kV, 40 mA, λ = 1.54187 Å) with a beam diameter of 0.5 mm and measured to 2θ = 40°. Single-crystal X-ray diffraction (SC-XRD) was measured on a Bruker APEX-II CCD diffractometer using Mo Kα radiation (λ = 0.71079 Å) equipped with an Oxford cryostream variable-temperature (VT) device. A single crystal was selected, and full data collections on the same crystal were made at 50 and 70 °C. Attempts to collect data at 90 °C led to sample decomposition. A second crystal was heated to 90 °C and then cooled to −100 °C. Data were collected using the Bruker APEX-II program,[19] integrated with SAINT,[20] and an absorption correction (SADABS)[21] was applied. The structure was solved using direct methods, and all atoms were refined anisotropically using full-matrix least-squares on F^2.[22] The structures of **1α** in the range −100 to +70 °C have been deposited with the CCCDC (CCCDC deposition numbers 1509435−1509437; the CIF files are also available as Supporting Information). Unit cell parameters and information on final residuals are presented in Table 1. Magnetic measurements were made on a Quantum Design MPMS SQUID magnetometer in dc mode in applied fields between 5 and 25 kOe in the range 1.8−45 K, while ac measurements were measured with a 10 Hz alternating field of 4.1 Oe. Additional magnetization vs field plots were collected at 1.8, 3.0, and 300 K. Heat capacity was measured on a pressed powder pellet fixed with Apiezon N grease on a Quantum Design PPMS. Tetrafluoroterephthalonitrile, p-$C_6F_4(CN)_2$, Li[N(SiMe$_3$)$_2$], and Ph_3Sb (Sigma-Aldrich) were used as received. SCl_2 was prepared according to the literature method.[23] Reactions were carried out under an argon atmosphere using dry solvents. Air-sensitive materials were handled in an MBraun LabMaster glovebox under a nitrogen atmosphere. Preparation of "crude" [**1**]Cl (ca. 90% purity by mass, contaminated with LiCl) followed the literature method,[24] and the product was isolated as a yellow solid in near-quantitative yield. Calculated yields of **1α** and **1β** assume pure [**1**]Cl, so true yields are higher than those reported.

Table 1. Single-Crystal Data for 1α at 50 and 70 °C, then Heating to 90 °C and Cooling to −100 °C

	temp/K		
	323(2)	343(2)	173(2) K
a/Å	7.712(1)	7.755(8)	7.5808(7)
b/Å	8.097(1)	8.13(1)	8.0566(7)
c/Å	9.705(2)	9.75(2)	9.5091(9)
α/deg	65.868(9)	65.7(1)	65.799(3)
β/deg	67.908(9)	67.56(9)	69.047(4)
γ/deg	67.474(9)	67.47(8)	67.515(3)
V/deg	493.3(1)	498(1)	475.36(8)
D_c/g·cm^{-3}	1.873	1.862	1.944
R(int)	0.036	0.058	0.023
R_1 ($I > 2\sigma(I)$)	0.061	0.072	0.063
wR_2 (all data)	0.142	0.205	0.187
S	1.294	1.185	1.207
residual e$^-$ density (e$^-$/Å^3)	+0.33	+0.48	+1.14
	−0.32	−0.31	−0.66

Preparation of 1. Triphenylantimony (0.281 g, 1.59 mmol) was added to solid [**1**]Cl (0.50 g, 1.6 mmol) under a nitrogen atmosphere. The mixture was heated at 50 °C for 30 min, leading to the formation of a black viscous oil. After the mixture cooled to room temperature, dichloromethane (10 mL) was added to afford a dark solution. After 10 min, the solvent was evaporated *in vacuo* to afford a dark residue, which was purified via sublimation onto a temperature-controlled cold-finger to afford either **1α** or **1β** as follows:

Sublimation under static vacuum (heated at 110 °C, substrate temperature +20 °C, 10^{-1} Torr) afforded black needle-shaped crystals of **1β** (0.35 g, 79%). Found: C, 34.19; N, 15.60. Calcd for $C_8F_4N_3S_2$: C, 34.53; N, 15.10.

Sublimation under static vacuum (heated at 110 °C, substrate temperature −10 °C, 10^{-1} Torr) afforded black flat block-shaped crystals of **1α** (0.28 g, 63%). Found: C, 33.70; N, 15.74. Calcd for $C_8F_4N_3S_2$: C, 34.53; N, 15.10%.

Both **1α** and **1β** were further characterized by solution EPR spectroscopy (g = 2.010, a_N = 5.06 G), and phase purity was confirmed by SC- and PXRD, DSC, IR, and Raman spectroscopy.

DOI: 10.1021/jacs.6b10707
J. Am. Chem. Soc. 2016, 138, 16779−16786

RESULTS AND DISCUSSION

The magnetic properties of **1β** have certainly proved worthy of study, yet the synthesis of **1** has been arduous. Although the synthesis of the intermediate dithiadiazolylium chloride salt [**1**]Cl appears to occur smoothly in good yield, recovered yields of crystalline **1β** from the subsequent 1e$^-$ reduction persistently proved poor (typically ca. 10%), despite our increasing experience with this radical over the past 20 years. Adjustments to the solvent (MeCN, THF, *l.* SO_2), reducing agent (Ag powder, Zn/Cu couple, $Na_2S_2O_4$, or Ph_3Sb), or reaction time did not markedly improve the recovered yields, rarely affording more than 150 mg of high-purity **1β** (based on 1.0 g of *p*-$C_6F_4(CN)_2$). Recently, Haynes reported an alternative "solvent-free" reduction method to prepare the closely related $[C_6F_5CNSSN]_2$ radical in 60% yield.[25] We therefore sought to exploit that methodology for the synthesis of **1**. When the yellow dithiadiazolylium chloride salt [**1**]Cl was heated at 50 °C with Ph_3Sb (mp 52−54 °C), a dark viscous oil formed, from which **1** could be sublimed as **1α** or **1β** (see below) in very good recovered yield (up to 79%) from the Ph_3SbCl_2 by-product (mp 143−145 °C). Notably, the volatility of **1** seems to preclude co-sublimation with Ph_3Sb, which has previously been shown to form a co-crystal with the DTDA radical, $[F_3CC_6H_4CNSSN]_2$.[26]

In order to evaluate the conditions necessary to selectively prepare **1α** and/or **1β** phases, we reviewed all our previous work in this area. We noted that the *α*-phase was most often prepared by inexperienced lab members who would heat the sample slowly, waiting for the first signs of sublimation, and collect the radical on a water-cooled cold-finger. With increased experience, the base temperature tended to be set slightly higher and the radical collected more rapidly on a water-cooled cold-finger or gradient-sublimed along a tube without external cooling, typically affording the *β*-phase. In many cases, the initial block-shaped crystals (**1α**) were replaced by needles (**1β**) during the sublimation process. Consequently, as students gained more laboratory experience, they became much more likely to make the *β*-phase, while those who were guided by experienced researchers often never made **1α** at all! Notably **1α** was more often made in the winter (Dec−Mar), although this also coincided with the prevalence of new, inexperienced lab members in that time period. In addition, we noted that, when **1β** was sublimed in high vacuum (90−0 °C, 10^{-6} Torr) in order to prepare thin films, **1α** was selectively formed.[27] From these accumulated observations, we speculated that **1α** was most likely to be formed when condensed at low temperatures and that **1** is most likely a poor thermal conductor, so slow sublimation onto a cold-finger would be desirable in order to maintain the surface temperature close to the water temperature (rationalizing the ability of inexperienced researchers to generate **1α**, especially in the winter when water supplies tend to be colder). In order to test this hypothesis, radical **1** was slowly vacuum-sublimed at 110 °C, with a cold-finger maintained at −10 °C using a temperature-controlled bath, and gratifyingly, pure **1α** was collected as black blocks in 63% recovered yield. Conversely, sublimation onto a cold-finger maintained at +10 °C (or higher) selectively afforded **1β** as long black needles (79%). The PXRD data on samples of **1α** and **1β** prepared in this fashion (Figure 1), coupled with DSC data and Raman spectroscopy (*vide infra*), confirmed the purity of both phases.

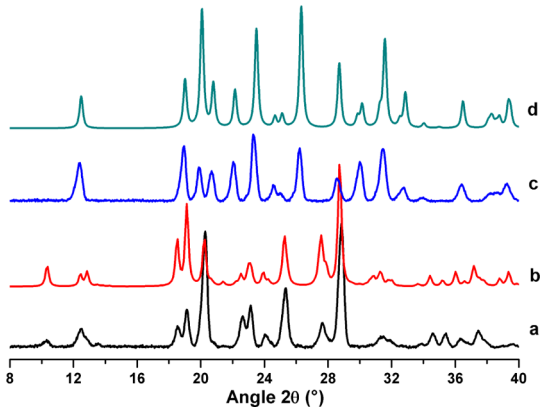

Figure 1. (a) Room-temperature PXRD data for **1α**. (b) Simulation of **1α** based on structure at 50 °C. (c) Room-temperature PXRD data for **1β**. (d) Simulation of **1β** based on the room-temperature structure of **1β** (CSD refcode: YOMXUT03).

Differential Scanning Calorimetry Studies. With high-purity **1α** and **1β** in hand, we were able to make a comparison of the relative stabilities of **1α** and **1β**. A summary of the thermodynamic data is presented in Table 2. In order to initiate this discussion, we will commence with DSC studies on **1β**. These revealed that the *β*-phase melts at 167−170 °C with ΔH_{fus} = +27 kJ·mol^{-1} (Figure 2a). The ΔH_{fus} value is somewhat lower than previously reported ΔH_{fus} values for dimeric DTDA radicals (36−62 kJ·mol^{-1}),[25] consistent with the observation that ΔH_{dim} typically contributes significantly to the overall lattice enthalpy. Upon cooling, recrystallization of liquid **1** occurs well below the melting point of **1β**, reflected in a sharp exotherm in the vicinity of 110−130 °C and dependent upon sample history. This behavior is not uncommon for viscous liquids.[28] Indeed, the metastable nature of the liquid phase below T_{mp} has previously been reported for several other thiazyl radicals.[18] A second reheating cycle reproduced essentially the same melting transition (164−168 °C), confirming that crystallization of **1** from the molten state afforded selectively **1β** (confirmed by PXRD).

Table 2. DSC Data Obtained in the Range −10 to 200 °C at Heating Rates of 10 °C·min^{-1} for the Phase Transitions of 1α and 1β

	transition temperature (°C)	ΔH (kJ·mol^{-1})
α-phase	54−66 (annealing)	−3
	111−117 (**1α** to **1β**)	+4
	167−170 (melt **1β**)	+27
β-phase	167−170	+27

The DSC trace for **1α** proved considerably more complex. Initial heating cycles typically revealed a small exothermic event in the region 54−66 °C (that was absent if the sample had previously been subjected to a heat−cool cycle to 90 °C). Both SC-XRD and PXRD studies revealed no evident change in structure (*vide infra*), and this exothermic transition can be attributed to thermal annealing of crystal defects, a feature observed in some other systems.[29] On heating above 100 °C, samples of **1α** initially exhibit an endothermic and irreversible transition at 111−117 °C, followed by a second endotherm at 167−170 °C (Figure 2). Both the temperature and enthalpy of fusion (+27 kJ·mol^{-1}) suggest that this latter transition can be

DOI: 10.1021/jacs.6b10707
J. Am. Chem. Soc. 2016, 138, 16779−16786

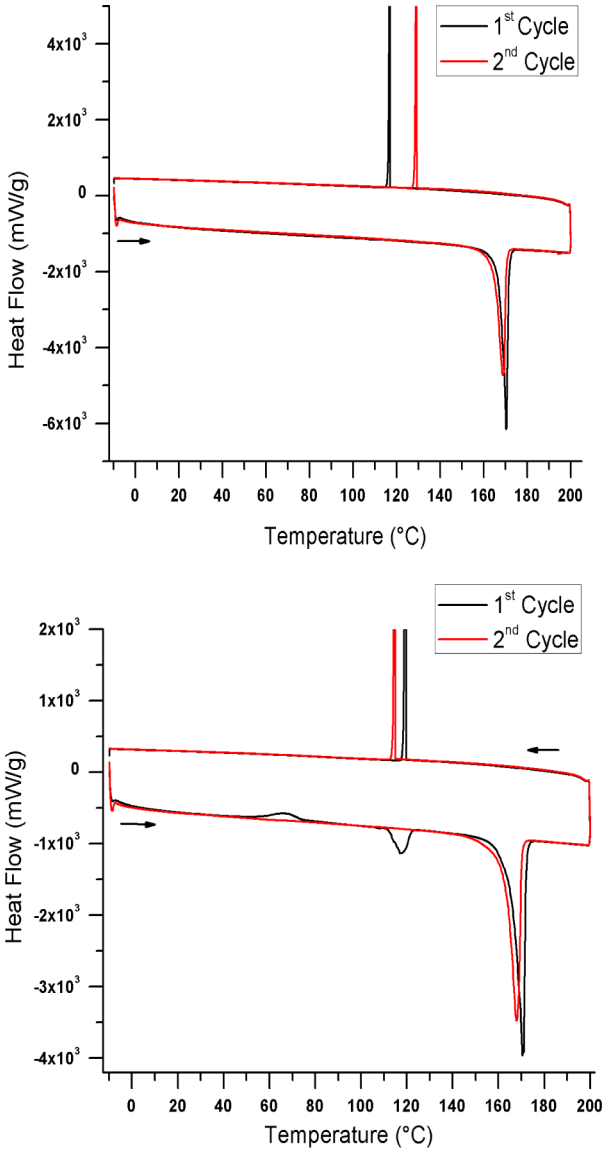

Figure 2. Differential scanning calorimetry on **1*β*** (top) and **1*α*** (bottom) measured from −10 to +200 °C at a heating rate of +10 °C·min^{-1} and a cooling rate of −5 °C·min^{-1}. Two cycles of heating and cooling were measured in both cases. The "spike" on the return cycle corresponds to crystallization of **1*β*** from the liquid phase.

assigned to melting of **1*β***, thereby suggesting that the irreversible transition in the range 111−117 °C is associated with a phase transition from **1*α*** to **1*β***. This was subsequently confirmed by VT PXRD studies (see below). The conversion of **1*α*** to **1*β*** is slightly endothermic (ΔH = +4 kJ·mol^{-1}), suggesting that the lattice enthalpy of **1*α*** is marginally more stable than that of **1*β*** and that transformation to **1*β*** is entropically favored. This is supported by calculated crystal densities [**1*α*** = 1.943 g·cm^{-3}, cf. **1*β*** = 1.894 g·cm^{-3} at 160(2) K] that conform to the density rule, which states that structures with higher density (more efficient packing) tend to have greater (enthalpic) stability.[30] VT PXRD studies (*vide infra*) confirmed the presence of crystalline **1*β*** rather than molten **1** in the region 117−170 °C.

Crystallographic Studies. In order to probe these phase transitions in more detail, VT PXRD studies on **1*α*** were undertaken on heating up to 130 °C. No significant change in the powder pattern of **1*α*** was observed up to 103 °C (Figure 3), consistent with a thermal annealing process rather than

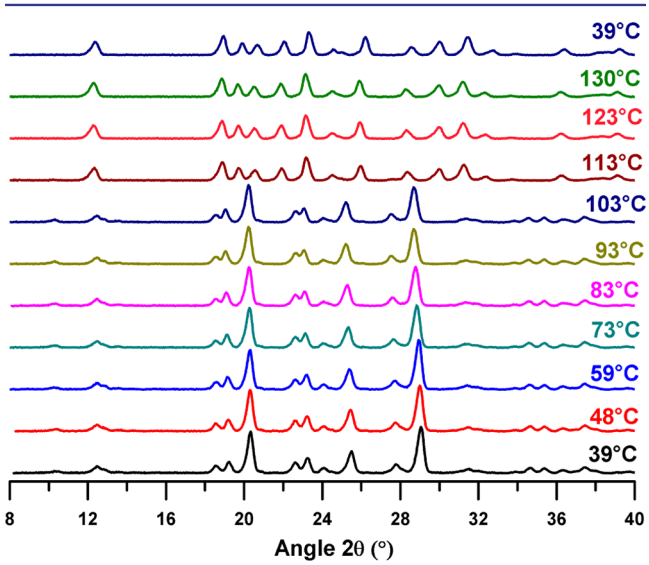

Figure 3. VT PXRD studies revealing conversion of **1*α*** to **1*β*** upon heating.

structural transition for **1*α*** in the vicinity of 54−66 °C. Further heating to 113 °C led to a marked change in the PXRD profile, consistent with conversion of **1*α*** to **1*β*** (DSC T_{onset} = 111 °C). From 113 to 130 °C, the PXRD profile remained unchanged, even after cooling, consistent with formation of **1*β***.

A SC-XRD study on **1*α*** has been reported previously.[12] However, VT SC-XRD studies on **1*α*** were undertaken to probe the structure of **1*α*** in more detail in the vicinity of the annealing temperature (54−66 °C) and as it approached the **1*α***−**1*β*** transition temperature (111 °C). Unit cell dimensions were measured across the range −100 to +90 °C and showed only the small changes expected for thermal expansion of the crystal lattice upon warming (see Supporting Information, SI-1), with no evident discontinuity expected for a phase transition. Structure determinations were made on the same single crystal at 50 and 70 °C, with crystal decomposition occurring at 90 °C. A second sample was heated to 90 °C and then immediately cooled to −100 °C, and a third data set was collected at −100 °C. These structure determinations revealed the structure to be **1*α*** in all cases. Structure refinement revealed some small increases in the magnitude of the thermal displacement parameters, U_{ij}, which appeared commensurate with the increasing temperature. There was no evidence for the onset of dynamic behavior or order/disorder in the vicinity of the transition around 54 °C, or upon further warming.

Crystals of **1*α*** adopt the triclinic space group $P\bar{1}$ and comprise chains of molecules linked through CN···S interactions parallel to [1 1 0]. Neighboring chains of molecules are related via a crystallographic inversion center (Figure 4, top). The structure of **1*β*** comprises similar supramolecular chains of molecules linked through CN···S interactions, but which now align co-parallel, affording a macroscopically polar structure (space group *Fdd*2, Figure 4, bottom). Thus, the transformation of **1*α*** to **1*β*** requires 50% of the molecules in the crystal to rotate by 180°, or all molecules to undergo a 90° reorientation. Although solid-state phase transitions are not uncommon in thiazyl radical chemistry,[31] such solid-state reactions typically occur with small net atomic displacements.[32]

DOI: 10.1021/jacs.6b10707
J. Am. Chem. Soc. 2016, 138, 16779−16786

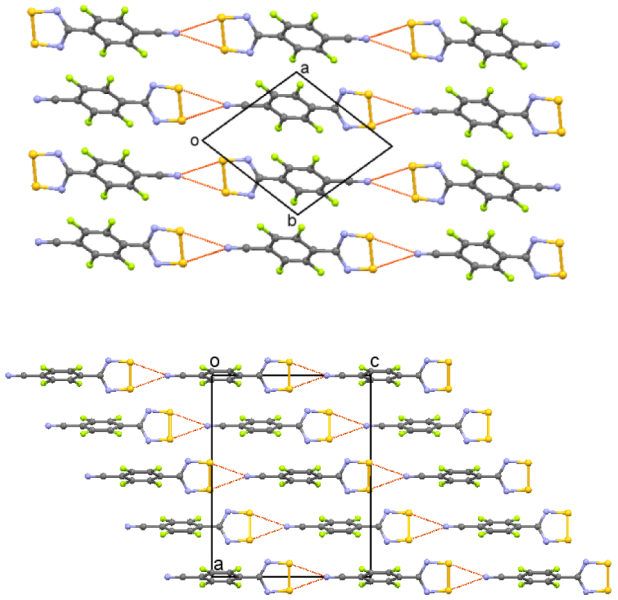

Figure 4. Crystal packing of **1*α*** (top) and **1*β*** (bottom).

More generally, other solid-state transformations, such as the topochemical [2+2] cycloaddition of alkenes,[33] have particularly well-defined geometric requirements for such solid-to-solid reactions.

The apparent transition from solid **1*α*** to solid **1*β*** at 111 °C therefore seemed unprecedented, given the drastic structural rearrangement required. An alternative conversion pathway may be for **1*α*** to melt and simultaneously recrystallize as **1*β***, a process which was examined through hot-stage microscopy studies.

Hot-Stage Microscopy. Samples of **1*α*** and **1*β*** were examined on a hot-stage microscope to optically probe the transitions evident in the DSC data. Both **1*α*** and **1*β*** are extremely dark solids, and so very thin blocks of **1*α*** were selected for these microscopy studies to permit some transmission of light through the sample. During the melt–recrystallization process, the material is spread even more thinly, and under these conditions **1*β*** appears yellow. On heating **1*α*** from room temperature to 105 °C, there was no marked change in morphology, although some sharpening of crystal features was observed (small crystallites on the surface disappeared), consistent with thermal annealing (Figure 5, top). On heating from 111 to 119 °C, a clear melt–recrystallization process was observed, with merger of individual crystals of **1*α*** to form polycrystalline **1*β*** (Figure 5, middle). No further change was then observed until 168 °C, when occlusions began to form and the melting of **1*β*** occurred (Figure 5, bottom).

Vibrational Spectroscopy. IR and Raman spectroscopies provide convenient tools for compound characterization through the presence of characteristic group vibrations, whereas the lower energy "fingerprint" region comprises more complex vibrations such as ring vibrations, wags, and bends that are characteristic of the molecule in question.[34] In particular, the fingerprint and low-energy regions of the IR/Raman spectra are sensitive to the nature of the polymorph present. In the current context, **1*α*** crystallizes in the low-symmetry triclinic space group $P\bar{1}$ with one molecule in the asymmetric unit, whereas **1*β*** adopts the orthorhombic space group *Fdd*2 with half a molecule in the asymmetric unit, i.e., rigorously C_2 symmetric. Raman spectroscopy in particular is sensitive to changes in the

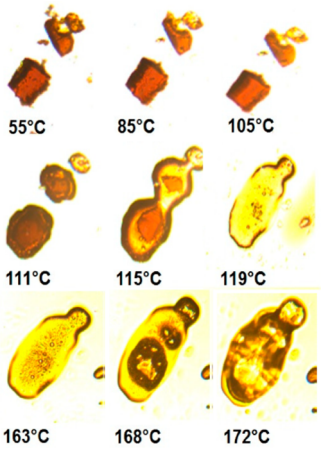

Figure 5. Hot-stage microscopy images of **1*α***: (top) annealing of **1*α***; (middle) melt–recrystallization **1*α*** to **1*β***; (bottom) melting of **1*β***.

crystal symmetry that can be reflected in band shifts, overall band splitting/coalescence, and/or changes to the relative peak intensity. Although **1*α*** and **1*β*** exhibit many peaks at very similar wavelengths, their relative intensities differ significantly (Figure 6), e.g., the $\nu_{C\equiv N}$ stretch at 2260 cm^{-1} is very strong for **1*β*** but rather weak for **1*α***.

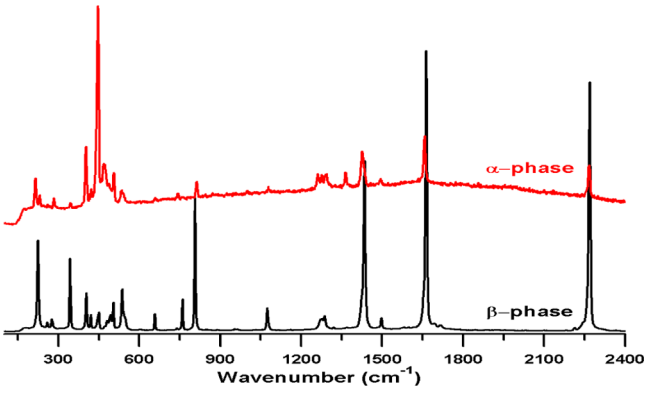

Figure 6. Comparison of the Raman spectra of **1*α*** (red) and **1*β*** (black).

An assignment of the vibrational spectrum is presented in SI-2. In the low-energy region (<300 cm^{-1}), **1*β*** is dominated by an intense peak at 224 cm^{-1}, whereas **1*α*** exhibits two peaks of lower intensity in this region (216 and 231 cm^{-1}), associated with an asymmetric C–C stretching vibration. A comparison of the IR and Raman data for **1*α*** and **1*β*** is available (SI-3).

Magnetic Studies. The magnetic properties of **1*β*** are now well documented, and the magnetic ordering of **1*β*** as a canted antiferromagnet at 36 K leads to a marked field dependence of the susceptibility in the low-temperature region.[7,14] Conversely, the magnetism of **1*α*** has not been thoroughly explored and requires phase-pure material in order to reliably determine the magnetic response of pristine **1*α*** in the low-temperature region below 36 K (where **1*β*** is magnetically ordered). The one previous study on high-purity **1*α***, measured on a Faraday balance (5–300 K), comprised a simple $\chi(T)$ plot that revealed a broad maximum in χ around 8 K, consistent with short-range antiferromagnetic interactions.[12] The absence of field-dependent studies, ac susceptibility measurements, or heat capacity experiments precluded any determination of whether long-

DOI: 10.1021/jacs.6b10707
J. Am. Chem. Soc. 2016, 138, 16779–16786

range order occurs in this phase. Recent theoretical studies of the magnetic exchange interactions in **1α** revealed competing ferro- and antiferromagnetic interactions (J = +10.9 and J' = −10.3 cm^{-1}) in the bc plane, which replicated the broad maximum in χ at 8 K.[35]

A sample of **1α** (62.7 mg), prepared by sublimation onto a cold (−10 °C) substrate and checked for phase purity by PXRD, was studied on a Quantum Design SQUID magnetometer in applied fields of 5, 10, 15, 20, and 25 kOe in the region 1.8−45 K. Additional ac data were collected in a 4.1 Oe field at 10 Hz. M vs H data were recorded at 1.8, 3.0, and 300 K (SI-4). A diamagnetic correction was applied to provide a best fit to Curie−Weiss behavior in the high-temperature region (χ_d = −0.00015 emu/mol, cf. value estimated from Pascal's constants, −0.00011 emu/mol).

Above 50 K, the material exhibits Curie−Weiss behavior, with C = 0.377 emu·K·mol^{-1} and θ = −3.8 K, indicative of weak antiferromagnetic interactions between S = 1/2 ions (Figure 7,

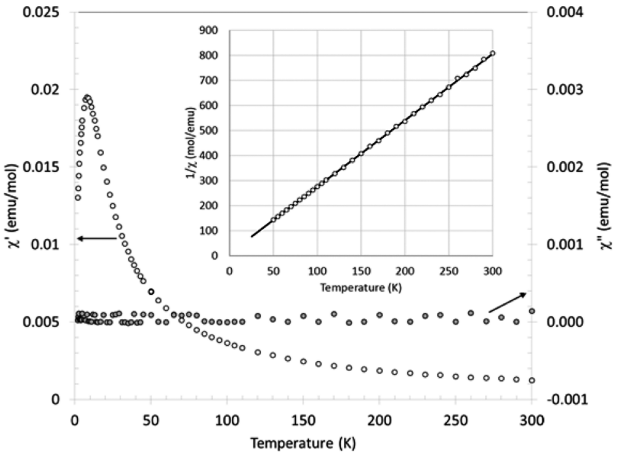

Figure 7. Temperature dependence of the ac susceptibility of **1α** in the region 1.8−300 K, with (inset) Curie−Weiss plot in the region 50−300 K.

inset). Upon cooling, a broad maximum in χ is observed around 8 K, consistent with previous observations. The absence of long-range order in the low-temperature regime is reflected in the absence of an out-of-phase component in the ac susceptibility, χ'' (Figure 7), and the presence of a broad feature in the heat capacity (see SI-5) characteristic of short-range order rather than a λ-type anomaly expected for a second-order magnetic phase transition.

Despite the absence of long-range order, some field dependence of the susceptibility was observed, with a divergence in susceptibility around 3 K as a function of applied field (Figure 8). The continued absence of features in either the ac data or heat capacity around 2 K suggests that such behavior is not associated with long-range order. In addition, M vs H plots on samples recorded at 1.8, 3.0, and 300 K reveal no evidence for ferromagnetic impurities or superparamagnetic particles (see SI-4). In order to understand the origin of the divergence in χ as a function of applied field, we returned to previous DFT studies of the exchange coupling in **1α**, in which two dominant exchange coupling pathways afford a chain motif with alternating ferro- and antiferromagnetic interactions (Figure 9).[35]

The magnetic properties of such S = 1/2 chains with alternating ferro- and antiferromagnetic interactions are

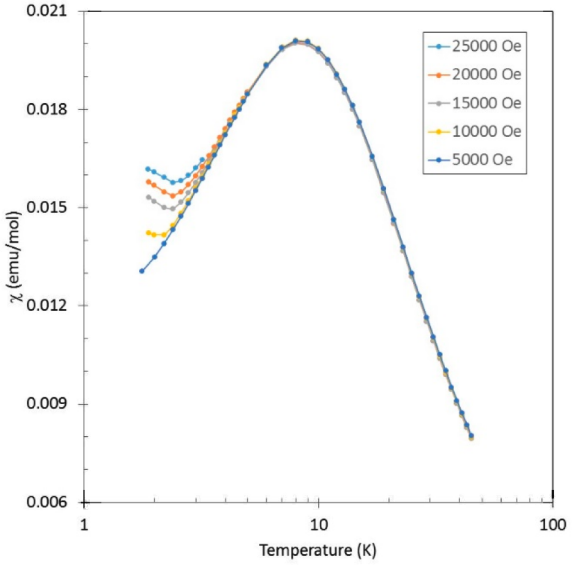

Figure 8. Field dependence of χ for **1α** in the region 1.8−45 K, with the temperature plotted on a log scale to highlight the divergence in the low-temperature region.

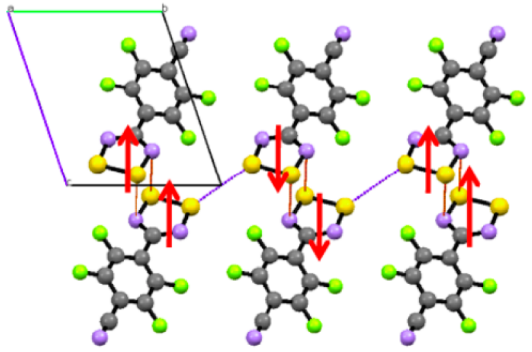

Figure 9. Idealized spin arrangement for **1α**, taking into account the chain-like magnetic topology arising from competing dominant ferromagnetic and antiferromagnetic exchange coupling.

sensitive to the nature of $|J/J'|$ as well as the anisotropy inherent in the system.[36] For radicals, the lack of significant orbital angular momentum leads to very small anisotropy, and previous studies on exchange-coupled DTDA dimers have revealed $|D| \approx 10^{-2}$ cm^{-1}.[37] Using the computed values of J and J', we find $|D/J| \rightarrow 0$ and $|J/J'| \approx 1$. Theoretically, these values of $|D/J|$ and $|J/J'|$ place it in a region which can be classified as a Haldane chain.[36] This affords an S_z = 0 ground state, which is separated from a band of low-lying triplet states (S_z = 0, ±1) by a finite energy gap Δ.[38] In small applied fields ($H < H_c$), then, the singlet ground state lies lowest in energy, and χ decreases exponentially to zero as $T \rightarrow 0$ K. In larger applied fields, the S_z = −1 term from the excited state becomes successively stabilized such that the energy gap decreases until a gapless state is formed.[38] In a qualitative sense, the magnetism of **1α** therefore reflects some form of gapped magnetic response, characterized by local minima in χ which are field-dependent. However, the system is likely somewhat far from an ideal Haldane system, as the chains are not completely isolated, with computed inter-chain interactions ca. 10% weaker than intra-chain ones.

DOI: 10.1021/jacs.6b10707
J. Am. Chem. Soc. 2016, 138, 16779−16786

CONCLUSIONS

Careful control of the sublimation conditions has permitted **1α** to be isolated in high purity. Thermal analysis and hot-stage microscopy supported by single-crystal and powder X-ray diffraction reveal that conversion of **1α** to **1β** between 111 and 117 °C occurs via a melt−recrystallization process. The endothermic nature of the transition indicates that **1β** is entropically favored over **1α** in the high-temperature regime. Magnetic studies on **1α** reveal a broad maximum in χ, diagnostic of short-range antiferromagnetic interactions. On cooling below χ_{max}, a field dependence of χ is observed, consistent with a gapped phase.

ASSOCIATED CONTENT

Supporting Information

The Supporting Information is available free of charge on the ACS Publications website at DOI: 10.1021/jacs.6b10707.

Crystal structures of **1α** at temperatures in the range 100−363 K (CIF)

SI-1 through SI-6, showing assignment of IR/Raman-active molecular vibrations of **1α** and **1β**, heat capacity of **1α**, *M* vs *H* plots on **1α**, additional DSC measurements on **1α**, and additional hot-stage microscopy images (PDF)

AUTHOR INFORMATION

Corresponding Authors

*palacio@unizar.es

*jmrawson@uwindsor.ca

ORCID

Jeremy M. Rawson: 0000-0003-0480-5386

Notes

The authors declare no competing financial interest.

ACKNOWLEDGMENTS

This article is dedicated to the many researchers who have worked on this radical over the past 20+ years at Durham and Cambridge Universities in the U.K. as well as at the University of Windsor (Canada). We thank NSERC for financial support through the Canada Research Chairs and RTI schemes and CFI/ORF for infrastructure support (J.M.R.) and NSERC Discovery program (M.P.). We also acknowledge support from grant MAT2015-68200-C2-2-P from the Ministerio de Economía y Competividad of Spain and the European Regional Development Fund. Additional support from Diputación General de Aragón (DGA-M4) is also acknowledged. Finally we would like to thank the reviewers for their constructive suggestions for revisions to this manuscript.

REFERENCES

(1) Tamura, M.; Nakazawa, Y.; Shiomi, D.; Nozawa, K.; Hosokoshi, Y.; Ishikawa, M.; Takahashi, M.; Kinoshita, M. *Chem. Phys. Lett.* **1991**, *186*, 401.

(2) (a) Chiarelli, R.; Novak, M. A.; Rassat, A.; Tholence, J. L. *Nature* **1993**, *363*, 147. (b) Kinoshita, M. *Jpn. J. Appl. Phys.* **1994**, *33*, 5718. (c) Miller, J. S. *Chem. Soc. Rev.* **2011**, *40*, 3266. (d) Cirujeda, J.; Mas, M.; Molins, E.; de Panthou, F. L.; Laugier, J.; Park, J. G.; Paulsen, C.; Rey, P.; Rovira, C.; Veciana, J. *J. Chem. Soc., Chem. Commun.* **1995**, 709. (e) *Magnetic Properties of Organic Materials*; Lahti, P., Ed.; Marcel Dekker: New York,1999. (f) *Molecular Magnetism: New Magnetic Materials*; Itoh, K., Kinoshita, M., Eds.; Gordon & Breach: Philadelphia, PA, 2000.

(3) (a) Allemand, P. M.; Khemani, K. C.; Koch, A.; Wudl, F.; Holczer, K.; Donovan, S.; Gruner, G.; Thompson, J. D. *Science* **1991**, *253*, 253. (b) Arcon, D.; Prassides, K. *Struct. Bonding (Berlin)* **2001**, *100*, 129.

(4) Rawson, J. M.; Alberola, A.; Whalley, A. *J. Mater. Chem.* **2006**, *16*, 2560.

(5) Blundell, S. *Magnetism in Condensed Matter*; Oxford University Press: Oxford, UK, 2001; p210.

(6) (a) Winter, S. M.; Hill, S.; Oakley, R. T. *J. Am. Chem. Soc.* **2015**, *137*, 3720. (b) Winter, S. M.; Oakley, R. T.; Kovalev, A. E.; Hill, S. *Phys. Rev. B: Condens. Matter Mater. Phys.* **2012**, *85*, 094430.

(7) (a) Banister, A. J.; Bricklebank, N.; Lavender, I.; Rawson, J. M.; Gregory, C. I.; Tanner, B. K.; Clegg, W.; Elsegood, M. R. J.; Palacio, F. *Angew. Chem., Int. Ed. Engl.* **1996**, *35*, 2533.

(8) Thomson, R. I.; Pask, C. M.; Lloyd, G. O.; Mito, M.; Rawson, J. M. *Chem. - Eur. J.* **2012**, *18*, 8629.

(9) Fujita, W.; Awaga, K. *Chem. Phys. Lett.* **2002**, *357*, 385.

(10) Fujita, W.; Awaga, K.; Nakazawa, Y.; Saito, K.; Sorai, M. *Chem. Phys. Lett.* **2002**, *352*, 348.

(11) Haynes, D. A. *CrystEngComm* **2011**, *13*, 4793.

(12) Banister, A. J.; Bricklebank, N.; Clegg, W.; Elsegood, M. R. J.; Gregory, C. I.; Lavender, I.; Rawson, J. M.; Tanner, B. K. *J. Chem. Soc., Chem. Commun.* **1995**, 679.

(13) Deumal, M.; Rawson, J. M.; Goeta, A. E.; Howard, J. A. K.; Copley, R. C. B.; Robb, M. A.; Novoa, J. J. *Chem. - Eur. J.* **2010**, *16*, 2741.

(14) Palacio, F.; Antorrena, G.; Castro, M.; Burriel, R.; Rawson, J. M.; Smith, J. N. B.; Bricklebank, N.; Novoa, J. J.; Ritter, C. *Phys. Rev. Lett.* **1997**, *79*, 2336.

(15) (a) Palacio, F.; Castro, M.; Antorrena, G.; Burriel, R.; Ritter, C.; Bricklebank, N.; Rawson, J.; Nicholas, J.; Smith, B. *Mol. Cryst. Liq. Cryst.* **1997**, *306*, 293. (b) Alberola, A.; Pask, C. M.; Rawson, J. M.; McInnes, E. J. L.; Wolowska, J.; El-Mkami, H.; Smith, G. M. *J. Phys. Chem. B* **2003**, *107*, 14158. (c) Pratt, F. L.; Goeta, A. E.; Palacio, F.; Rawson, J. M.; Smith, J. N. B. *Phys. B* **2000**, *289-290*, 119.

(16) (a) Miller, J. S. *Adv. Mater.* **1998**, *10*, 1553. (b) Leznoff, D. B.; Rancurel, C.; Sutter, J.-P.; Rettig, S. J.; Pink, M.; Paulsen, C.; Kahn, O. *J. Chem. Soc., Dalton Trans.* **1999**, 3593. (c) Akpinar, H.; Mague, J. T.; Novak, M. A.; Friedman, J. R.; Lahti, P. M. *CrystEngComm* **2012**, *14*, 1515. (d) Tao, J.; Wei, R.-J.; Huang, R.-B.; Zheng, L. S. *Chem. Soc. Rev.* **2012**, *41*, 703. (e) Fettouhi, M.; Ouahab, L.; Hagiwara, M.; Codjovi, E.; Kahn, O.; Constant-Machado; Varret, F. *Inorg. Chem.* **1995**, *34*, 4152. Zhang, L.; Song, T.; Xu, J.; Sun, J.; Zeng, S.; Wu, Y.; Fan, Y.; Wang, L. *CrystEngComm* **2014**, *16*, 2440.

(17) (a) Dunitz, J. D.; Bernstein, J. *Acc. Chem. Res.* **1995**, *28*, 193. (b) Bucar, D. K.; Lancaster, R. W.; Bernstein, J. *Angew. Chem., Int. Ed.* **2015**, *54*, 6972.

(18) (a) Brooks, W. V. F.; Burford, N.; Passmore, J.; Schriver, M. J.; Sutcliffe, L. H. *J. Chem. Soc., Chem. Commun.* **1987**, 69. (b) Du, H.; Haddon, R. C.; Krossing, I.; Passmore, J.; Rawson, J. M.; Schriver, M. J. *Chem. Commun.* **2002**, 1836.

(19) *APEX2*, Version 2008.1-0; Bruker AXS Inc.; Madison, WI, 2008.

(20) *SAINT*, Data Reduction Software, V6.28A; Bruker AXS Inc.; Madison, WI, 2001.

(21) Sheldrick, G. M. *SADABS*, Program for Empirical Absorption Correction; University of Gottingen: Gottingen, Germany, 1996.

(22) Sheldrick, G.M. *SHELXL-97*, Program for the Refinement of Crystal; 2012.

(23) Fehér, F. In *Handbook of Preparative Inorganic Chemistry*, 2nd ed., Vol. *1*; Brauer, G., Ed.; Academic Press: New York, 1963; p 371.

(24) (a) Beldjoudi, Y.; Haynes, D. A.; Hayward, J. J.; Manning, W. J.; Pratt, D. R.; Rawson, J. M. *CrystEngComm* **2013**, *15*, 1107. (b) Alberola, A.; Carter, E.; Constantinides, C. P.; Eisler, D. J.; Murphy, D. M.; Rawson, J. M. *Chem. Commun.* **2011**, *47*, 2532.

(25) Robinson, S. W.; Haynes, D. A.; Rawson, J. M. *CrystEngComm* **2013**, *15*, 10205.

(26) Boeré, R. T. *CrystEngComm* **2016**, *18*, 2748.

DOI: 10.1021/jacs.6b10707
J. Am. Chem. Soc. 2016, 138, 16779−16786

(27) Caro, J.; Fraxedas, J.; Santiso, J.; Figueras, A.; Rawson, J. M.; Smith, J. N. B.; Antorrena, G.; Palacio, F. *Thin Solid Films* **1999**, *352*, 102.
(28) Ubbelohde, A. R. *The Molten State of Matter*; John Wiley: Chichester, England, 1978.
(29) (a) Feng, T.; Pinal, R.; Carvajal, M. T. *J. Pharm. Sci.* **2008**, *97*, 3207. (b) Butterhof, C.; Martin, T.; Ectors, P.; Zahn, D.; Niemietz, P.; Senker, J.; Näther, C.; Breu, J. *Cryst. Growth Des.* **2012**, *12*, 5365.
(30) (a) Kitaigorodskii, I. *Organic Chemical Crystallography*; Consultants Bureau: New York, 1961. (b) Bernstein, J. *Polymorphism in Molecular Crystals*; Oxford University Press: Oxford, UK, 2007.
(31) (a) Aherne, C.; Banister, A. J.; Luke, A. W.; Rawson, J. M.; Whitehead, R. J. *J. Chem. Soc., Dalton Trans.* **1992**, 1277. (b) Fujita, W.; Awaga, K. 1999, *286*, 261. (c) Alberola, A.; Collis, R. J.; Humphrey, S. M.; Less, R. J.; Rawson, J. M. *Inorg. Chem.* **2006**, *45*, 1903. (d) Brusso, J. L.; Clements, O. P.; Haddon, R. C.; Itkis, M. E.; Leitch, A. A.; Oakley, R. T.; Reed, R. W.; Richardson, J. F. *J. Am. Chem. Soc.* **2004**, *126*, 8256. (e) Suizu, R.; Iwasaki, A.; Shuku, Y.; Awaga, K. *J. Mater. Chem. C* **2015**, *3*, 7968.
(32) Kohlschütter, V.; Haenni, P. *Z. Anorg. Allg. Chem.* **1918**, *105*, 121.
(33) (a) Biradha, K.; Santra, R. *Chem. Soc. Rev.* **2013**, *42*, 950. (b) Hayward, J. J.; Gumbau-Brisa, R.; Clarke, C.; Alberola, A.; Rawson, J. M.; Pilkington, M. *CrystEngComm* **2014**, *16*, 7268.
(34) (a) Brillante, A.; Bilotti, I.; Della Valle, R. G.; Venuti, E.; Girlando, A. *CrystEngComm* **2008**, *10*, 937. (b) Lebedkin, S.; Blum, C.; Stürzl, N.; Hennrich, F.; Kappes, M. *Rev. Sci. Instrum.* **2011**, *82*, 013705. (c) Carteret, C.; Dandeu, A.; Moussaoui, S.; Muhr, H.; Humbert, B.; Plasari, E. *Cryst. Growth Des.* **2009**, *9*, 807. (d) Surovtsev, V. N.; Malinovsky, K. V.; Boldyreva, V. E. *J. Chem. Phys.* **2011**, *134*, 045102.
(35) Deumal, M.; LeRoux, S.; Rawson, J. M.; Robb, M. A.; Novoa, J. J. *Polyhedron* **2007**, *26*, 1949.
(36) Hida, K. *Phys. Rev. B: Condens. Matter Mater. Phys.* **1992**, *46*, 8268.
(37) (a) Cameron, T. S.; Decken, A.; Kowalczyk, R. M.; McInnes, E. J. L.; Passmore, J.; Rawson, J. M.; Shuvaev, K. V.; Thompson, L. K. *Chem. Commun.* **2006**, 2277. (b) Decken, A.; Cameron, T. S.; Passmore, J.; Rautiainen, J. M.; Reed, R. W.; Shuvaev, K. V.; Thompson, L. K. *Inorg. Chem.* **2007**, *46*, 7436. (c) Decken, A.; Ebdah, M.; Kowalczyk, R. M.; Landee, C. P.; McInnes, E. J. L.; Passmore, J.; Shuvaev, K. V.; Thompson, L. K. *Inorg. Chem.* **2007**, *46*, 7756. (d) Shuvaev, K. V.; Decken, A.; Grein, F.; Abedin, T. S. M.; Thompson, L. K.; Passmore, J. *Dalton Trans.* **2008**, 4029. (e) Constantinides, C. P.; Eisler, D. J.; Alberola, A.; Carter, E.; Murphy, D. M.; Rawson, J. M. *CrystEngComm* **2014**, *16*, 7298.
(38) Maeda, Y.; Hotta, C.; Oshikawa, M. *Phys. Rev. Lett.* **2007**, *99*, 057205.

DOI: 10.1021/jacs.6b10707
J. Am. Chem. Soc. 2016, 138, 16779−16786